⌘ *Author's Choice*

Proteomics Analysis of the Cardiac Myofilament Subproteome Reveals Dynamic Alterations in Phosphatase Subunit Distribution*[S]

Xiaoke Yin‡§, Friederike Cuello‡§¶, Ursula Mayr‡, Zhiqi Hao‖, Martin Hornshaw, Elisabeth Ehler‡, Metin Avkiran‡, and Manuel Mayr‡ ‡‡**

Myofilament proteins are responsible for cardiac contraction. The myofilament subproteome, however, has not been comprehensively analyzed thus far. In the present study, cardiomyocytes were isolated from rodent hearts and stimulated with endothelin-1 and isoproterenol, potent inducers of myofilament protein phosphorylation. Subsequently, cardiomyocytes were "skinned," and the myofilament subproteome was analyzed using a high mass accuracy ion trap tandem mass spectrometer (LTQ Orbitrap XL) equipped with electron transfer dissociation. As expected, a small number of myofilament proteins constituted the majority of the total protein mass with several known phosphorylation sites confirmed by electron transfer dissociation. More than 600 additional proteins were identified in the cardiac myofilament subproteome, including kinases and phosphatase subunits. The proteomic comparison of myofilaments from control and treated cardiomyocytes suggested that isoproterenol treatment altered the subcellular localization of protein phosphatase 2A regulatory subunit B56α. Immunoblot analysis of myocyte fractions confirmed that β-adrenergic stimulation by isoproterenol decreased the B56α content of the myofilament fraction in the absence of significant changes for the myosin phosphatase target subunit isoforms 1 and 2 (MYPT1 and MYPT2). Furthermore, immunolabeling and confocal microscopy revealed the spatial redistribution of these proteins with a loss of B56α from Z-disc and M-band regions but increased association of MYPT1/2 with A-band regions of the sarcomere following β-adrenergic stimulation. In summary, we present the first comprehensive proteomics data set of skinned cardiomyocytes and demonstrate the potential of proteomics to unravel dynamic changes in protein composition that may contribute to the neurohormonal regulation of myofilament contraction. ***Molecular & Cellular Proteomics 9: 497–509, 2010.***

Myofilament proteins comprise the fundamental contractile apparatus of the heart, the cardiac sarcomere. They are subdivided into thin filament proteins, including actin, tropomyosin, the troponin complex (troponin C, troponin I, and troponin T), and thick filament proteins, including myosin heavy chains, myosin light chains, and myosin-binding protein C. Although calcium is the principal regulator of cardiac contraction through the excitation-contraction coupling process that culminates in calcium binding to troponin C, myofilament function is also significantly modulated by phosphorylation of constituent proteins, such as cardiac troponin I (cTnI),[1] cardiac myosin-binding protein C (cMyBP-C), and myosin regulatory light chain (MLC-2). "Skinned" myocyte preparations from rodent hearts, in which the sarcolemmal envelope is disrupted through the use of detergents, have been invaluable in providing mechanistic information on the functional consequences of myofilament protein phosphorylation following exposure to neurohormonal stimuli that activate pertinent kinases prior to skinning or direct exposure to such kinases in active form after skinning (for recent examples, see studies on the phosphorylation of cTnI (1–3), cMyBP-C (4–6), and MLC-2 (7–9)). Nevertheless, to date, only a few myofilament proteins have been studied using proteomics (10–19), and a detailed proteomic characterization of the myofilament subproteome and its associated proteins from skinned myocytes has not been performed. In the present analysis, we used an LTQ Orbitrap XL equipped with ETD (20) to analyze the subproteome of skinned cardiomyocytes with or without prior stimulation. Endothelin-1 and isoproterenol were used to activate the endothelin receptor/protein kinase C and β-adrenoreceptor/protein kinase A pathway, respectively (21, 22). Importantly, the mass accuracy of the Orbitrap mass analyzer helped to distinguish true phosphorylation sites from false assignments, and the sensitivity of the ion trap provided novel insights

From the ‡King's British Heart Foundation Centre, King's College London, London SE5 9NU, United Kingdom, ‖ThermoFisher Scientific, San Jose, California 95134, United States and **ThermoFisher Scientific, Stafford House, Boundary Way, Hemel Hempstead HP2 7GE, United Kingdom

⌘ *Author's Choice*—Final version full access.

Received, June 19, 2009, and in revised form, December 22, 2009

Published, MCP Papers in Press, December 27, 2009, DOI 10.1074/mcp.M900275-MCP200

[1] The abbreviations used are: cTnI, cardiac troponin I; ET1, endothelin-1; ETD, electron transfer dissociation; LTQ, linear trap quadrupole; ISO, isoproterenol; mmu, millimass units; MYPT, myosin phosphatase target subunit isoform; PP, protein phosphatase; PTM, post-translational modification; cMyBP-C, cardiac myosin-binding protein C; MLC-2, myosin regulatory light chain; BES, 2-[bis(2-hydroxyethyl)amino]ethanesulfonic acid; IPI, International Protein Index; MHC, myosin heavy chain.

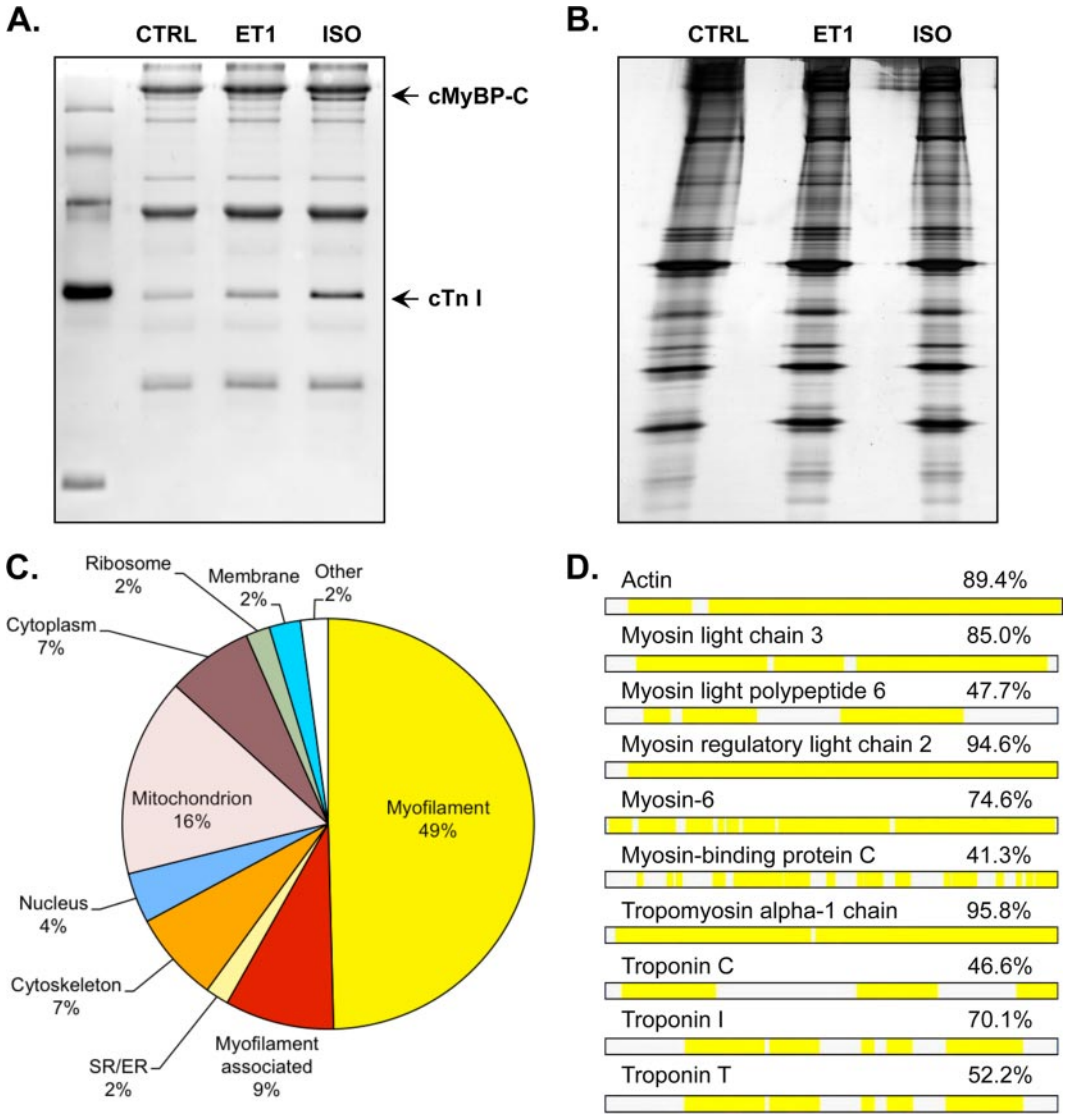

FIG. 1. **Myofilament subproteome.** *A*, increased intensity of the ProQ Diamond staining indicates phosphorylation of cTnI and cMyBP-C upon exposure to ET1 (5 nM) or ISO (10 nM) for 10 min (3). *B*, protein composition of the myofilament subproteome in vehicle (*CTRL*), ET1, and ISO groups after silver staining. *C*, myofilament proteins and myofilament-associated proteins constituted 58% of all spectra identified. *D*, sequence coverage of representative myofilament proteins obtained by MS/MS. *ER*, endoplasmic reticulum; *SR*, sarcoplasmic reticulum.

into the translocation of phosphatase regulatory and targeting subunits following β-adrenergic stimulation.

EXPERIMENTAL PROCEDURES

Isolation and Culture of Adult Ventricular Myocytes—Rat or mouse ventricular myocytes were isolated from the hearts of male Wistar rats or C57B mice (body weight, 200–250 or 20–25 g, respectively; B&K Universal Ltd.) by collagenase-based enzymatic digestion as described previously (3). In brief, hearts were excised from terminally anesthetized and heparinized (60 mg/kg sodium pentobarbitone and 100 units of sodium heparin intraperitoneally) animals and initially perfused for 5 min with modified HEPES-Krebs solution (pH 7.3 at 37 °C) containing 130 mmol/liter NaCl, 4.5 mmol/liter $MgCl_2$, 0.4 mmol/liter NaH_2PO_4, 0.75 mmol/liter $CaCl_2$, 4.2 mmol/liter HEPES, 20 mmol/liter taurine, 10 mmol/liter creatine, and 10 mmol/liter glucose. Hearts were then consecutively perfused with Ca^{2+}-free HEPES-Krebs solution containing 100 μmol/liter EGTA (4 or 10 min) and HEPES-Krebs solution containing 100 μmol/liter $CaCl_2$ and 1 mg/ml type II collagenase (Worthington) (8 or 4 min). All solutions were gassed with 100% O_2 and maintained at 37 °C. Hearts were then removed from the perfusion apparatus, the ventricles were cut into small pieces, and the pieces were incubated in 30 or 10 ml of the collagenase solution gassed with 100% O_2 for a further 7 or 4 min at 37 °C. Isolated myocytes were separated from undigested ventricular tissue by filtering through nylon gauze, and the latter was incubated in 30 or 10 ml of the collagenase solution for a further 8 min. This step was repeated, thereby generating three isolated myocyte fractions. In each fraction, myocytes were allowed to settle into a loose pellet, and the supernatant was removed and replaced with HEPES-Krebs solution containing 1% BSA and 500 μmol/liter $CaCl_2$. Myocytes were again allowed to settle, the supernatant was removed, and the cells were finally pooled and resuspended in 30 or 10 ml of HEPES-Krebs

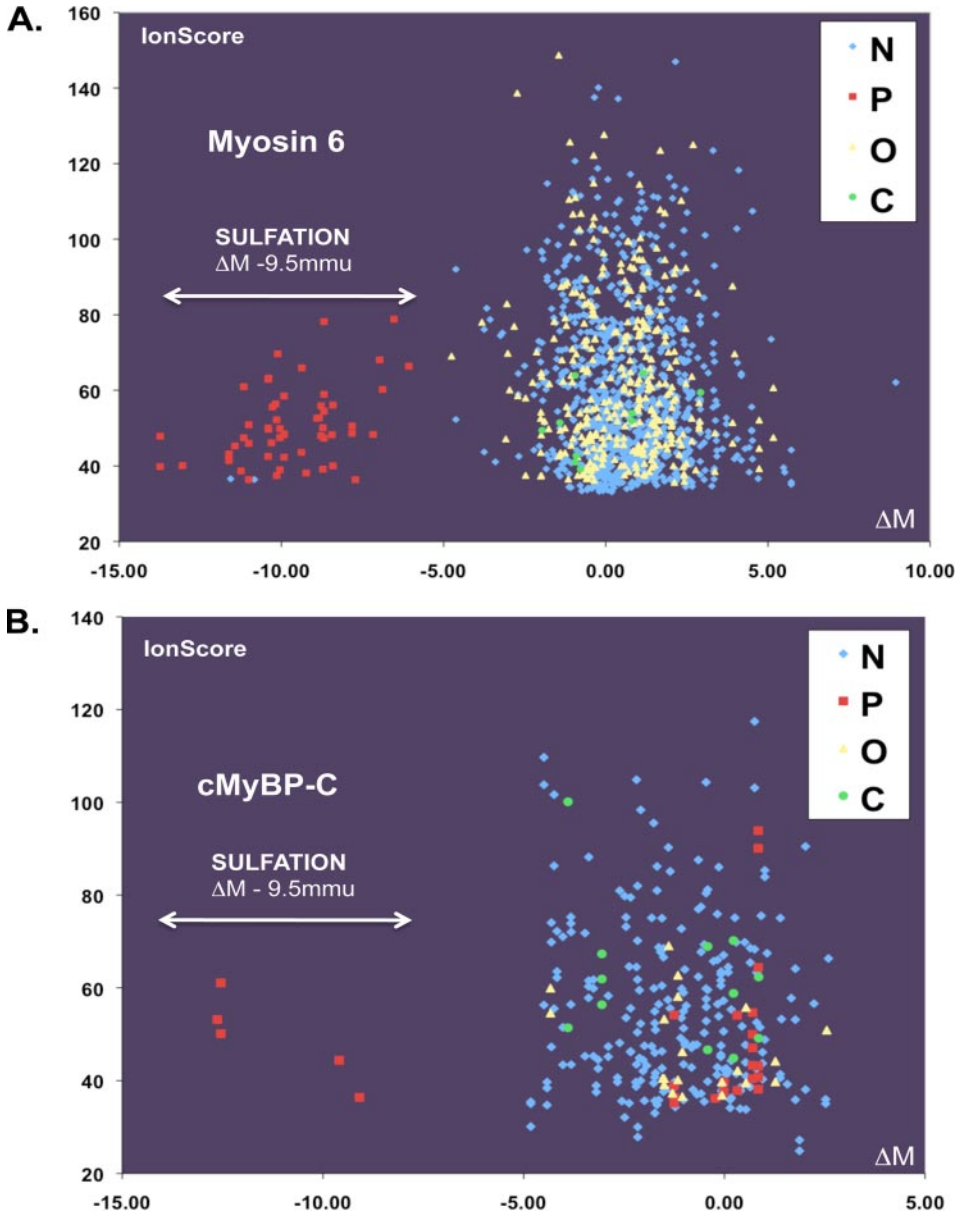

FIG. 2. **Phosphorylation of myofilament proteins.** MS/MS data were analyzed by Proteome Discoverer using the MASCOT algorithm. The mass error of the parent ion (Δ*M*, mmu) was plotted against the ion score. For myosin-6, most peptides with neutral loss showed a mass error of −9.5 mmu indicative of sulfation (*A*). For myosin-binding protein C, only neutral loss precursors with accurate mass represented true phosphorylation sites (*B*). Search results for MS/MS spectra are as follows: *N* denotes no PTMs; *P*, phosphorylation of serine, threonine, and tyrosine; *O*, oxidation of methionine; *C*, carboxymethylation of cysteine.

solution containing 1 mmol/liter $CaCl_2$. The pooled isolated myocytes were pelleted by brief centrifugation at 50 × *g* and washed at room temperature with modified M199 culture medium (Invitrogen) containing 2 mmol/liter creatine, 2 mmol/liter carnitine, and 5 mmol/liter taurine plus 100 IU/ml penicillin/streptomycin. Following further centrifugation at 50 × *g*, myocytes were again resuspended in modified M199 medium. Myocytes were then pipetted into the prelaminated wells of plastic 6-well culture plates for protein subfractionation, Western immunoblot analysis, and gel-LC-MS/MS or on individual 3.5-cm dishes for immunocytochemistry and confocal microscopy and allowed to adhere for 90 min in an incubator (37 °C, 5% CO_2). The culture medium was replaced with fresh modified M199 medium, and the cells were maintained overnight.

Pharmacological Treatment and Chemical Permeabilization of Ventricular Myocytes—Endothelin-1 (ET1) was from Calbiochem, and isoproterenol (ISO) was from Sigma-Aldrich. After exposure to vehicle, ET1 (5 nmol/liter), or ISO (10 nmol/liter) for 10 min, myocytes were chemically permeabilized (skinned) as described previously (3) by suspension in relaxing solution (pH 7.1 at 25 °C) containing 70 mmol/liter potassium propionate, 100 mmol/liter BES, 10 mmol/liter disodium phosphocreatine, 6.3 mmol/liter Na_2H_2ATP, 1 mmol/liter $MgCl_2$, 10 mmol/liter K_2EGTA, and 1 mmol/liter DTT (total ionic strength, 200 mmol/liter) with added 1% Triton X-100. Myocytes were kept at 4 °C during the skinning procedure. After 15 min, the myocytes were washed briefly in PBS and fixed for 10 min with 4% paraformaldehyde in PBS for immunocytochemistry ex-

periments or solubilized in sample loading buffer (Invitrogen) for gel-LC-MS/MS.

Immunolabeling of Skinned Myocytes—Skinned myocytes were incubated in 5% nonspecific goat serum in 1% BSA, TBS (pH 7.5) containing 20 mmol/liter Trizma (Tris base), 155 mmol/liter NaCl, 2 mmol/liter EGTA, and 2 mmol/liter $MgCl_2$ for 20 min. Primary and secondary antibodies were diluted using 1% BSA, TBS. Incubation with primary antibodies was carried out overnight at 4 °C; incubation with secondary antibodies was carried out at room temperature for 4 h. After final washing with PBS, the skinned myocytes were mounted with coverslips in 0.1 M Tris-HCl (pH 9.5), glycerol (3:7) including 50 mg/ml *n*-propyl gallate as an antifading reagent (23).

Antibodies and Fluorescent Reagents—The monoclonal mouse anti-sarcomeric myosin heavy chain (clone 10F5-s) antibody was obtained from the Developmental Studies Hybridoma Bank maintained at the University of Iowa and was used at a dilution of 1:50. The monoclonal rabbit antibody to myosin phosphatase target subunit isoforms 1 and 2 (MYPT1/2) was from Abcam and was used at a dilution of 1:100 for immunocytochemistry and 1:1000 for Western immunoblotting. The monoclonal mouse anti-B56α antibody was from BD Transduction Laboratories and was used at a dilution of 1:1000 for Western immunoblotting. The polyclonal rabbit anti-protein phosphatase 2A (PP2A) B′ (B56) subunit antibody was from Millipore and was used at a dilution of 1:200 for immunocytochemistry. The glyceraldehyde-3-phosphate dehydrogenase horseradish peroxidase-conjugated antibody was from Abcam and was used at a dilution of 1:5000. The polyclonal rabbit anti-cardiac troponin I antibody was from Cell Signaling Technology and was used at a dilution of 1:1000. The monoclonal mouse anti-Na,K-ATPase α1 antibody was from Millipore and was used at a dilution of 1:10,000. For double immunofluorescence labeling, a combination of Cy3-conjugated anti-mouse (1:500) and Cy5-conjugated anti-rabbit (1:100) secondary antibodies was used. The secondary antibodies were purchased from Jackson ImmunoResearch Laboratories. 4′,6-Diamidine-2-phenylindole dihydrochloride (1 mg/ml 1:100) was purchased from Sigma.

Confocal Microscopy—The specimens were analyzed using confocal microscopy on an inverted microscope (Leica SP5 system, Mannheim, Germany) equipped with a blue diode and argon and helium neon lasers using a 63×/1.4 numerical aperture oil immersion lens.

Adult Rat Ventricular Myocyte Subfractionation—Myocytes were subfractionated as described previously (24). In brief, myocytes were lysed in ice-cold lysis buffer (pH 7.5) containing 50 mmol/liter Tris-HCl, 5 mmol/liter EGTA, 2 mmol/liter EDTA, 5 mmol/liter DTT as well as 0.05% digitonin and protease inhibitor mixture (Roche Applied Science). The samples were frozen by floating the culture plate on a volume of liquid N_2 and thawed at room temperature. Cell lysates were then centrifuged at 14,000 × *g* for 30 min at 4 °C, and the supernatant, which comprised the cytosolic fraction, was removed. The pellet was then solubilized in an equal volume of the digitonin-based lysis buffer containing 1% Triton X-100 and centrifuged at 14,000 × *g* for 30 min at 4 °C, and the supernatant, which comprised the membrane fraction, was removed. The remaining Triton-insoluble pellet contained the myofilament fraction. Equal volumes of Laemmli sample buffer were added to all three fractions prior to immunoblot analysis.

Immunoblot Analysis—Immunoblot analysis was carried out as described previously (3, 25). In brief, the fractionated protein samples were resolved by 7.5, 10, or 15% SDS-PAGE; transferred to polyvinylidene difluoride membranes; and subjected to immunoblotting. Primary antibodies were detected by donkey anti-rabbit or sheep anti-mouse secondary antibodies linked to horseradish peroxidase (GE Healthcare). Specific protein bands were detected by enhanced chemiluminescence. The bands were scanned on a calibrated densi-

TABLE I

Phosphorylation sites as confirmed by electron transfer dissociation and accurate mass of the precursor ion

Bold underlined "s," phosphorylation of serine; bold underlined "m," oxidation of methionine; MS2, fragmentation method; Delta mass, mass accuracy of the precursor ion; Ctrl, control myofilaments.

Protein name	Accession no.	Peptide sequence	PTM	MS2	Observed *m/z*	Delta mass	*z*	Mascot score	Mascot Expect	Group
						mmu				
Myosin-binding protein C, cardiac	IPI00118316.2	RT**s**LAGAGR	Ser-273	CID	484.73669	−1.25	2	54	1.20e−04	Ctrl
		RT**s**LAGAGR	Ser-273	ETD	484.73669	−1.25	2	36	6.90e−03	Ctrl
		T**s**LAGAGR	Ser-273	ETD	406.68665	−0.23	2	36	6.80e−03	Ctrl
		RT**s**LAGAGR	Ser-273	CID	484.73767	0.70	2	55	1.00e−04	ISO
		RT**s**LAGAGR	Ser-273	ETD	484.73767	0.70	2	50	3.00e−04	ISO
		T**s**LAGAGR	Ser-273	ETD	406.68692	0.32	2	54	1.10e−04	ISO
		RT**s**DSHEDAGTLDFSSLLK	Ser-282	CID	720.32690	0.84	3	43	3.30e−03	ISO
		RT**s**DSHEDAGTLDFSSLLK	Ser-282	ETD	720.32690	0.84	3	94	2.80e−08	ISO
		T**s**DSHEDAGTLDFSSLLK	Ser-282	ETD	1001.93573	−0.01	2	40	6.40e−03	ISO
Isoform 1 of tropomyosin α-1	IPI00123316.1	AISEELDHALND**m**T**s**I	Ser-283	ETD	927.89374	−2.59	2	47	1.10e−03	Ctrl
Troponin I, cardiac muscle	IPI00223197.5	RR**ss**ANYR	Ser-23, Ser-24	ETD	585.23370	−1.15	2	25	6.40e−02	ISO

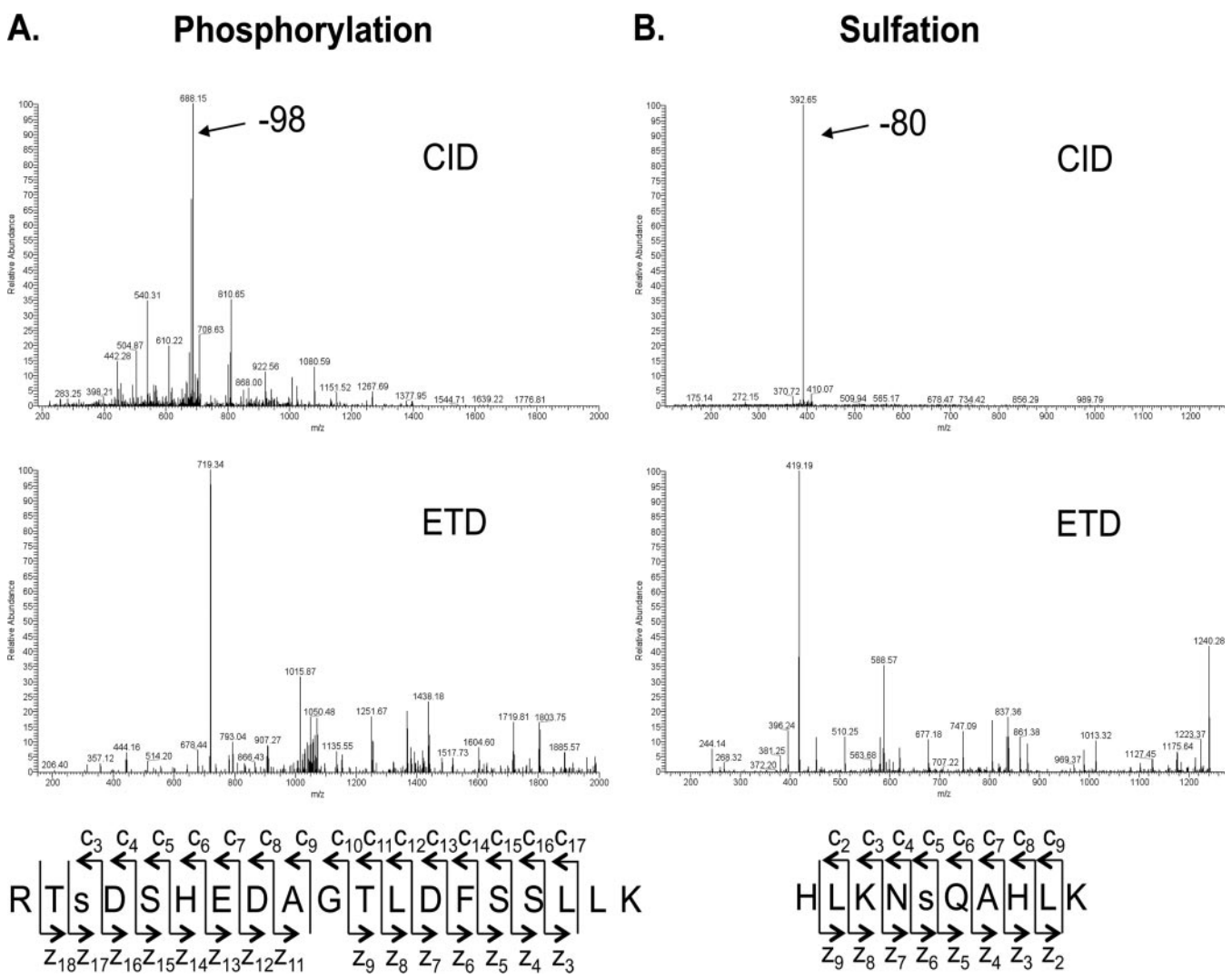

FIG. 3. **Fragmentation spectra of sulfated and phosphorylated peptides.** Shown are CID MS/MS and ETD MS/MS spectra of a phosphorylated peptide (*A*) and a sulfated peptide (*B*). A neutral loss of ~32.5 was observed for a triply charged precursor at *m/z* 720.66, which is equivalent to a loss of 98 (*A*), whereas a neutral loss of ~26.6 was observed for the triply charged precursor at *m/z* 419.19, which is equivalent to a loss of 80 (*B*). For detailed annotation of the product ion spectra, please refer to supplemental Fig. 1.

tometer (GS-800, Bio-Rad) and normalized to the total protein content following Coomassie staining of the membrane using Image Quant TL (GE Healthcare) software, and -fold changes in response to treatment were expressed as the percentage of its own control.

ProQ Diamond Staining—Skinned myofilament proteins were separated on 15% acrylamide gels and fixed in 50% methanol, 10% acetic acid overnight at room temperature. After washing with water (three times for 15 min), gels were stained with ProQ Diamond phosphoprotein stain (Molecular Probes) for 3 h in the dark (26). The gels were destained four times for 40 min with 4% ACN, 50 mM sodium acetate (pH 4.0) and subsequently scanned on a Typhoon 9400 Imager (GE Healthcare) with an excitation wavelength of 532 nm and a 580-nm long pass emission filter.

Gel-LC-MS/MS—Samples were denatured with 2× sample loading buffer (Invitrogen) at 96 °C for 5 min and then separated in 5–20% polyacrylamide gels with 5% stacking gels on top at 3 watts per gel for 18 h. After SDS-PAGE, gels were stained using the PlusOne Silver staining kit (GE Healthcare) with slight modifications (27). Silver staining was used for band excision to avoid cross-contamination with faint gel bands. Coomassie staining only visualizes the abundant myofilament proteins but does not show the fainter gel bands in between. Although the entire gel lane was excised and no "empty" gel pieces were left behind, it is important for the quantitation by mass spectrometry that the gel bands are excised precisely to ensure equal loading in each LC-MS/MS experiment. Tryptic in-gel digestion was performed using the Investigator ProGest (Genomic Solutions) robotic digestion system with sequencing grade modified trypsin (Promega) (28, 29). Following enzymatic degradation, rat samples were separated by liquid chromatography on a reverse-phase column (C_{18} PepMap100, 3 μm, 100 Å, 25 cm; Dionex) and applied to an LTQ Orbitrap XL mass spectrometer (Thermo Scientific). Spectra were collected from the mass analyzer using full ion scan mode over the *m/z* range 300–2000. Six dependent MS/MS scans were performed on each ion using dynamic exclusion. The murine samples were separated by liquid chromatography on a reverse-phase column and applied to an LTQ Orbitrap XL mass spectrometer equipped with ETD (Thermo Scientific). Spectra were collected from the mass analyzer using full ion scan mode over the *m/z* range 400–2000. Six dependent

TABLE II
Spectral counts for kinases and phosphatases identified in the myofilament subproteome
C1–3, control myofilaments 1–3. Spectral counts are the number of assigned spectra. SH3, Src homology 3.

	Accession no.	Molecular mass	C1	C2	C3
		kDa			
Signaling kinases and associated proteins					
cAMP-dependent protein kinase catalytic subunit α	KAPCA_RAT	41	4	4	0
cAMP-dependent protein kinase type I-α regulatory subunit	KAP0_RAT	43	12	14	0
cAMP-dependent protein kinase type II-α regulatory subunit	KAP2_RAT	46	6	6	0
Nucleoside-diphosphate kinase B	NDKB_RAT	17	31	35	10
Putative myosin light chain kinase 3	MYLK3_MOUSE	86	6	6	6
SH3 domain-containing kinase-binding protein 1	SH3K1_RAT	78	6	7	0
Striated muscle-specific serine/threonine-protein kinase	SPEG_RAT	354	14	20	34
Phosphatases					
Low molecular weight phosphotyrosine-protein phosphatase	PPAC_RAT	18	13	10	0
Protein phosphatase 1 regulatory subunit 12A	MYPT1_RAT	115	9	12	0
Protein phosphatase 1 regulatory subunit 12B	MYPT2_MOUSE	109	46	28	23
Serine/threonine-protein phosphatase 2A 56-kDa regulatory subunit α isoform	2A5A_MOUSE	56	9	9	10
Serine/threonine-protein phosphatase 2A 65-kDa regulatory subunit A α isoform	2AAA_MOUSE	65	24	24	8
Serine/threonine-protein phosphatase PP1β catalytic subunit	PP1B_RAT	37	12	17	8

MS/MS scans (three CIDs and three ETDs) were performed on each ion using dynamic exclusion.

Protein Identification—The MS/MS data obtained from the rat cardiac myofilaments were matched to a combined rat (7419 protein entries), mouse (16,177 protein entries), and human (20,332 protein entries) database (UniProt/Swiss-Prot, release version 15.7) using the SEQUEST version 28 (revision 13) (BioWorks version 3.3.1 SP1, Thermo Scientific) algorithm. Carboxyamidomethylation of cysteine was used as a fixed modification, and oxidation of methionine was used as a variable modification. The mass tolerance was set at 10 ppm for the precursor ions and at 1 AMU for fragment ions. One missed cleavage was allowed. An initial search against the entire UniProt/Swiss-Prot database returned nearly all identifications as mouse or rat proteins. Certain peptides (*e.g.* of rat α-actinin 2), however, displayed greater sequence homology to the human than the mouse protein. Hence, we focused the search on a combined mouse/rat/human database, which is still substantially larger than the entire rodent database. By reducing the database size, all LC-MS/MS experiments could be merged, and protein and peptide probabilities could be computed using Scaffold software (version 2.5.0, Proteome Software). Assignments were accepted with >99.9% protein probability, >95.0% peptide probability, and a minimum of two peptides (30, 31). For the purpose of quantitative testing, nine biosamples were generated from three independent experiments (three controls, three ET-1, and three ISO). At least 48 LC-MS/MS experiments were acquired per biosample. Scaffold software (version 2.5.0, Proteome Software) was used to assign the spectral counts across individual biosamples and categories (controls, ET-1, and ISO). For the murine samples, the database searches were performed using MASCOT version 2.0 (32) (Proteome Discoverer 1.0, Thermo Scientific) against the IPI mouse database (version 3.47, 55,298 protein entries). Carboxyamidomethylation of cysteine was used as a fixed modification. Oxidation of methionine and phosphorylation of serine, threonine, and tyrosine were used as variable modifications. The mass tolerance for the precursor ions was set at 10 ppm. The mass tolerance of fragment ions was set at 0.8 Da for CID and 1.2 Da for ETD. One missed cleavage was allowed. The following filter criteria were applied: expectation value <0.05 and at least two peptides per protein.

Statistical Analysis—Statistical analysis was performed using the Student's *t* test or analysis of variance and Scheffe's post hoc test. A *p* value of <0.05 was considered significant.

RESULTS

Characterization of Cardiac Myofilament Subproteome—Ventricular myocytes from adult rat hearts were treated with vehicle, endothelin-1, or isoproterenol. The latter is a β-adrenoreceptor agonist that induces phosphorylation of several known myofilament proteins, such as cTnI and cMyBP-C, through the cAMP-dependent protein kinase pathway. Following stimulation, the myocytes were skinned using established protocols (3) to disrupt membranes and deplete cytosolic proteins. The remaining proteins in the skinned cardiomyocytes, containing predominantly myofilament and myofilament-associated proteins, were extracted in Laemmli buffer and separated by one-dimensional SDS-PAGE. Staining of the gels with the phosphoprotein stain ProQ Diamond confirmed robust phosphorylation of cTnI and cMyBP-C following isoproterenol treatment (Fig. 1*A*). Parallel one-dimensional gels were silver-stained (Fig. 1*B*), and gel bands were excised and digested with trypsin. Peptides were separated on a reverse-phase column by nanoflow HPLC interfaced to an LTQ Orbitrap XL tandem mass spectrometer. In control myofilaments, 613 proteins were identified in at least two of three biological replicates with a minimum of two unique peptides. The entire MS/MS data set is deposited in PRIDE

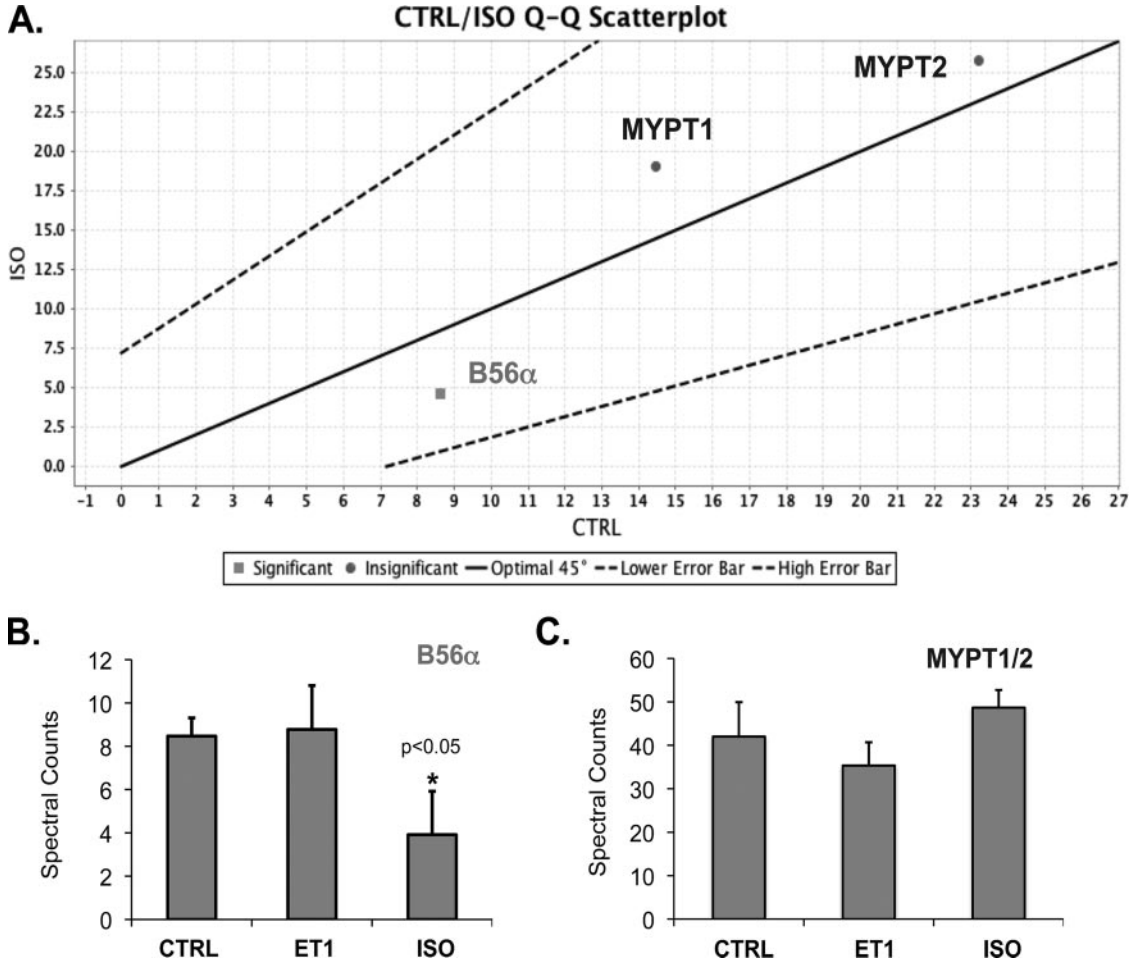

FIG. 4. **Phosphatase translocation as revealed by spectral counting.** The Q-Q scatterplot displays the relative change in phosphatase regulatory subunits between control and ISO stimulation (*A*). Proteins that lie along the *45° line* have the same number of spectral counts between the two categories. Note the significant reduction of PP2A B56α, whereas MYPT1 and MYPT2 remain above the *45° line*. Changes in the assigned spectral count of PP2A B56α (*B*) and MYPT1 and MYPT2 upon ET-1 and ISO stimulation (*C*) are shown. Data are derived from $n = 3$ samples for control (*CTRL*), endothelin, and isoproterenol treatment, respectively (total, $n = 9$) and expressed as means $\pm$ S.E. * denotes significant difference from controls and ET-1.

the proteomics identifications database (http://www.ebi.ac.uk/pride/ under accession numbers 10137–10292). For the full lists of identified proteins and peptides, please refer to supplemental Tables 1 and 2. Based on the spectral count, 23 myofilament proteins constituted the majority of the total protein mass (Fig. 1*C*). For these proteins, high sequence coverage was obtained (Fig. 1*D*), and several of the CID spectra showed a neutral loss of 80 or 98.

Phosphorylation of Myofilament Proteins—Subsequent analysis using CID and ETD focused on gel bands containing myofilament proteins from murine cardiomyocytes to take advantage of the comprehensive protein database that is available for this species for the assignment of post-translational modifications. Numerous positive hits were returned when phosphorylation of serine, threonine, and tyrosine was assigned as a variable PTM for the myofilament proteins. In agreement with previous reports (PhosphoSitePlus) only precursors measured with a mass accuracy of less than 5 mmu were phosphopeptides (Fig. 2, Table I, and supplemental Fig. 1). These precursors also had CID MS/MS spectra containing intense, neutral loss ions corresponding to a loss of 98 (Fig. 3*A*). In contrast, precursor ions with a mass deviation of approximately -9.5 mmu (Fig. 2) were consistent with sulfation of serine, threonine, or tyrosine residues, and their CID MS/MS spectra contained neutral loss ions corresponding to a loss of 80 (Fig. 3*B*), a potential pitfall in phosphopeptide assignment (33). The accurate mass measurement of the precursor ion in the Orbitrap mass analyzer with parallel CID MS/MS measurement in the linear ion trap readily discriminated sulfation from phosphorylation. However, ETD measurement gave more discrimination in terms of localizing the site of the peptide modification with five phosphorylation sites identified by ETD, whereas only two were identified by CID (Table I).

Phosphatase Translocation in Myofilament Subproteome—The analysis of the myofilament subproteome has led to iden-

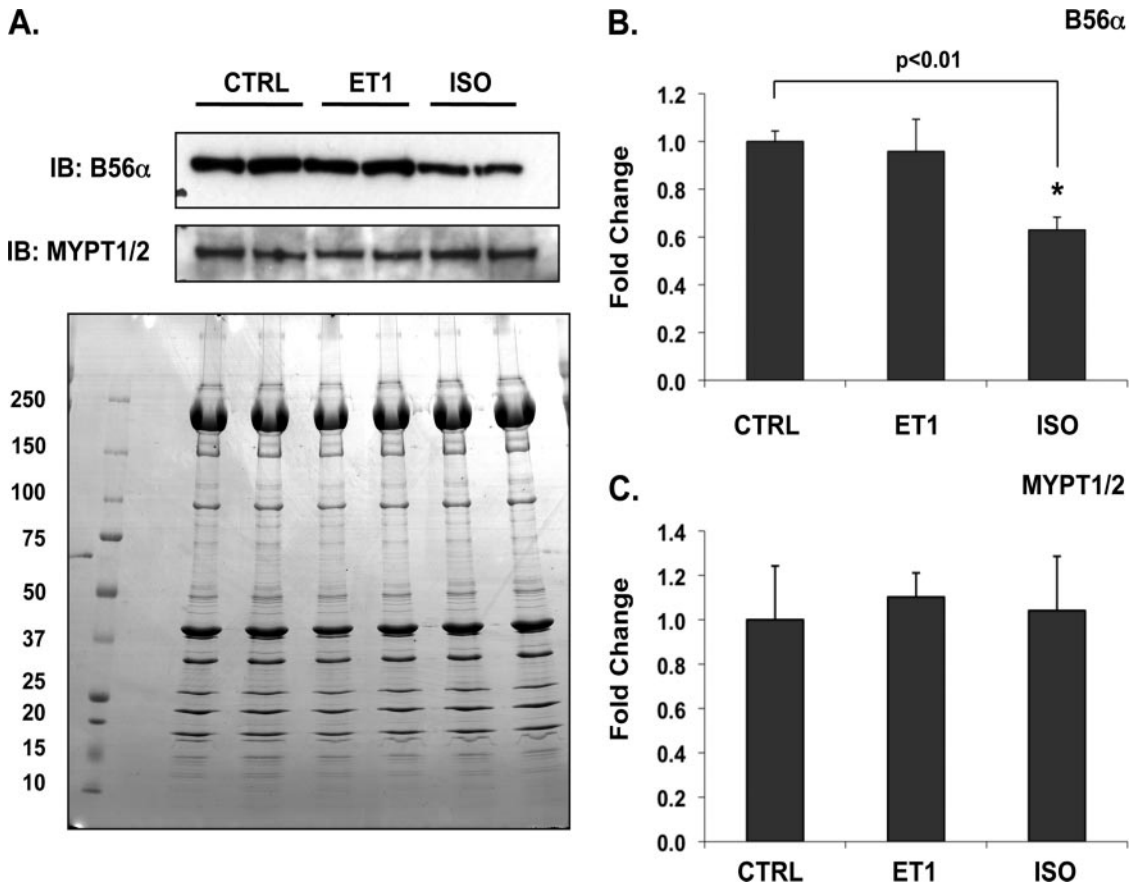

FIG. 5. **Validation by immunoblotting.** Immunoblot (*IB*) analysis of ventricular myocytes exposed to vehicle (*CTRL*), 5 nM ET1, or 10 nM ISO for 10 min prior to harvesting is shown. Myofilament extracts were probed for PP2A B56α and MYPT1/2 (*A*, *upper panel*). Coomassie staining confirmed equal loading (*A*, *lower panel*). The relative change compared with controls as quantified by densitometry of immunoblots for PP2A B56α (*B*) and MYPT1/2 (*C*) is shown. Data are derived from $n = 4$ samples per group and expressed as means $\pm$ S.E. * denotes significant difference from controls.

tifications of scarce proteins including kinases and phosphatases (Table II). Intriguingly, a comparison between control and isoproterenol-treated samples suggested dynamic changes in phosphatase regulatory subunits: a quantile-quantile (Q-Q) scatterplot displays the relative change between the two categories (Fig. 4*A*). According to the spectral counts based on three biological replicates per group, β-adrenergic stimulation by isoproterenol for 10 min was sufficient to decrease the myofilament content of the PP2A regulatory subunit B56α (Fig. 4*B*) in the absence of significant changes for the MYPT1 and MYPT2 (Fig. 4*C*). These data suggest a translocation of phosphatase regulatory subunits to the non-myofilament compartment after a short time course of stimulation with isoproterenol.

To substantiate these observations using independent methodology, immunoblotting on myofilament extracts was performed and confirmed that treatment with isoproterenol, but not endothelin-1, substantially modified the B56α content of the myofilament subproteome (Fig. 5, *A–C*), providing independent confirmation of the spectral count data presented in Fig. 4, *A–C*. The subsequent focus was on isoproterenol treatment: we fractionated myocytes into cytosolic, membrane, and myofilament fractions following stimulation with vehicle or isoproterenol. We followed established protocols to obtain cytosolic, membrane, and myofilament fractions for subsequent immunoblot analysis (24). The selected markers for different myocyte compartments, glyceraldehyde-3-phosphate dehydrogenase (cytosolic), Na,K-ATPase α1 subunit (membrane), and cTnI (particulate/myofilament), exhibited their expected localization, reflecting successful subcellular fractionation (Fig. 6*A*). Immunoblot analysis of the B56α content of subcellular fractions revealed it to be increased in the cytosolic fraction (250% of untreated control) and decreased in the myofilament fraction (15% of control) following isoproterenol treatment. The opposite profile was observed when a similar analysis was conducted using an antibody that recognizes both MYPT1 and MYPT2 with a decrease in the MYPT content of the cytosolic fraction (10% of control) and a modest increase in the MYPT content of the myofilament fraction following isoproterenol treatment (150% of control), demonstrating that the apparent isoproterenol-induced changes in phosphatase regulatory subunits within the myofilament compartment reflected specific trans-

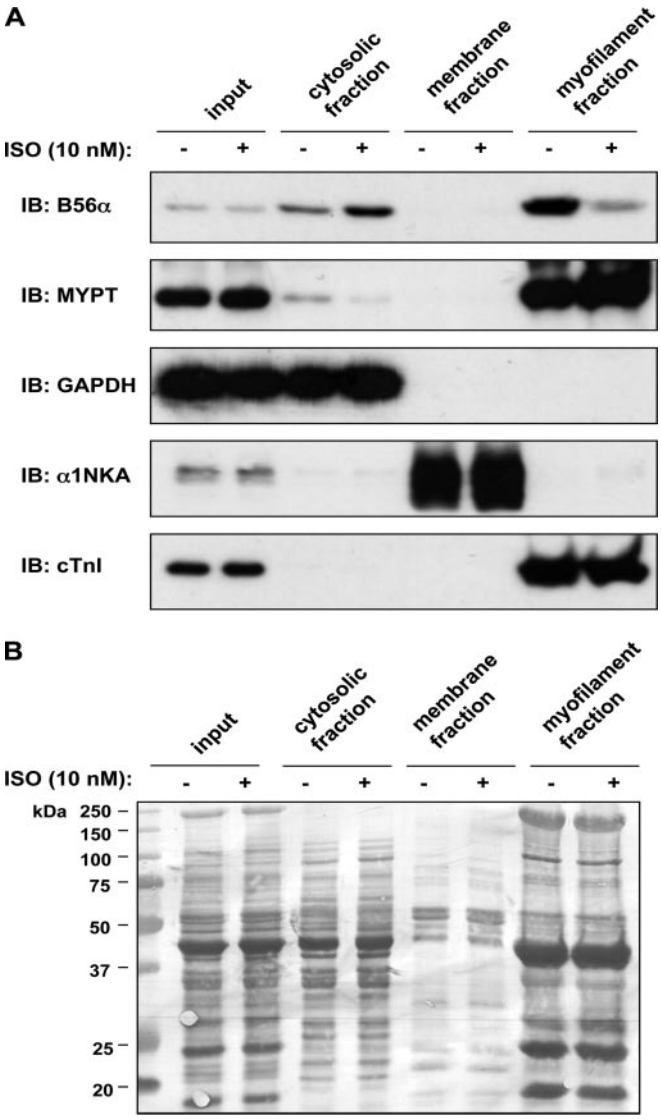

FIG. 6. **Protein analysis of myocyte fractions.** Ventricular myocytes were exposed to vehicle (−) or ISO (+). Representative immunoblots (*IB*) of total lysate (*input*) and cytosolic, membrane, and myofilament fractions were probed for B56α, MYPT1/2, glyceraldehyde-3-phosphate dehydrogenase (*GAPDH*), Na,K-ATPase α1 subunit (α*1NKA*), or cTnI (*A*). Coomassie staining of the membranes (*B*) revealed the total protein content of the samples analyzed in *A*. Results are representative of two independent experiments.

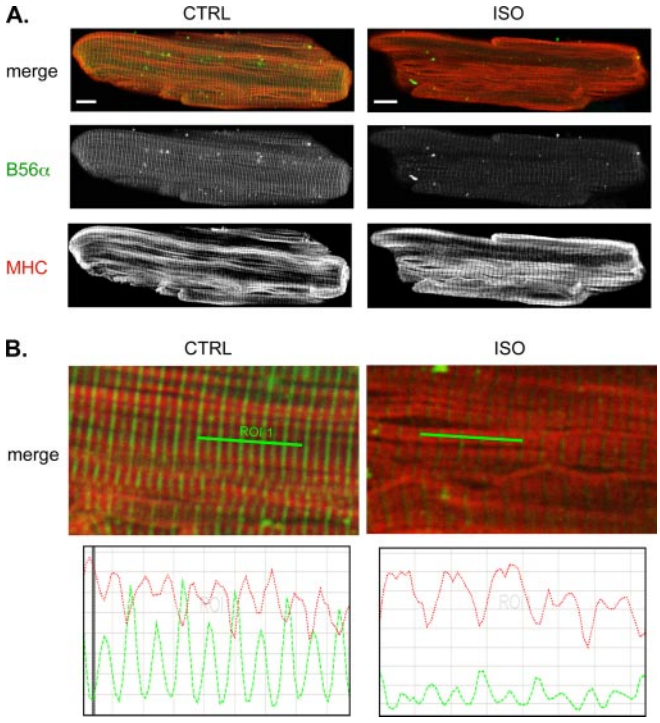

FIG. 7. **Localization of B56α in sarcomere.** *A*, images of cultured adult rat ventricular myocytes chemically permeabilized after exposure to vehicle (*CTRL*) or 10 nM ISO for 10 min. B56α and sarcomeric MHC were labeled with specific antibodies (*green* and *red*, respectively). *Scale bar*, 10 μm. *B*, *top panels*, high magnification sections of merged images from *A*. *Bottom panels*, fluorescence intensity histograms taken from the indicated region of interest (*ROI*), highlighting the localization of B56α (*green line*) in Z-disc and M-band regions and between the A-band regions populated by sarcomeric MHC (*red line*) and the reduced intensity of the signal for B56α (*green line*) in both these regions after β-adrenergic stimulation.

location events in these proteins. Coomassie-stained membranes are shown as additional controls (Fig. 6*B*).

Confocal Microscopy to Obtain Spatial Information—Although the proteomics and immunoblot analyses indicated that redistribution of phosphatase regulatory and targeting subunits occurred in response to β-adrenergic stimulation, these techniques did not reveal the exact distribution of these proteins within the sarcomeric lattice. Therefore, we immunolabeled B56α or MYPT1/2 in skinned myocytes and explored their sarcomeric localization by confocal microscopy. B56α was found to reside in the Z-disc and M-band regions and was lost from both regions following isoproterenol treatment (Fig. 7). In contrast, MYPT1/2 exhibited predominantly an intrasarcomeric translocation in response to β-adrenergic stimulation and was also localized to the Z-disc and M-band regions in the basal state but moved to co-localize with myosin heavy chain (MHC) head regions at A-band regions following isoproterenol treatment (Fig. 8). Thus, our proteomics analysis not only comprehensively characterized skinned cardiomyocytes (Fig. 9*A*) but also revealed translocation of myofilament-associated phosphatase regulatory and targeting subunits upon β-adrenergic stimulation (Fig. 9*B*).

DISCUSSION

Our study demonstrates that skinned cardiomyocytes represent a promising subproteome amenable for investigation using label-free quantitation and validates the utility of proteomics analysis in identifying dynamic changes in myofilament composition. The concept of using skinned cardiomyocytes for proteomics analysis could be important for the wider application of proteomics in cardiac research as cardiomyo-

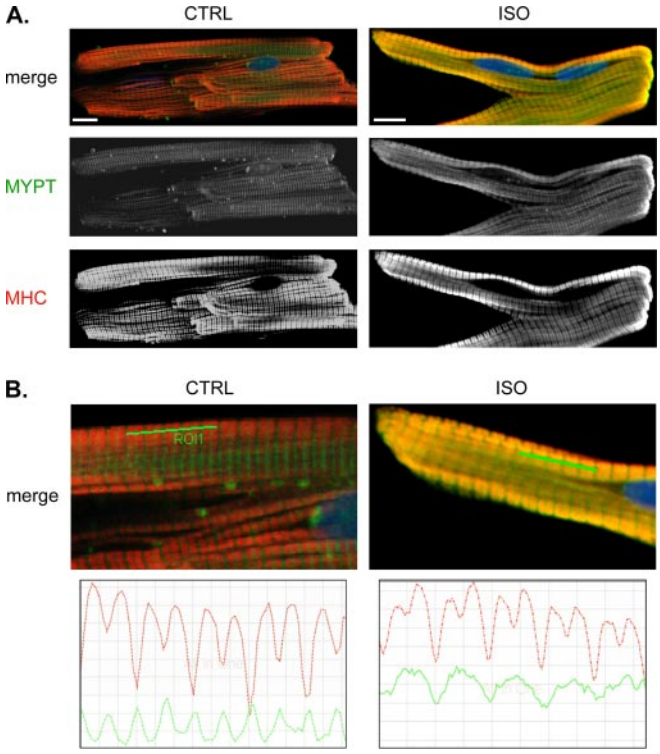

FIG. 8. **Localization of MYP1/2 in sarcomere.** *A*, images of cultured adult rat ventricular myocytes chemically permeabilized after exposure to vehicle (*CTRL*) or 10 nM ISO for 10 min. MYPT1/2 and sarcomeric MHC were labeled with specific antibodies (*green* and *red*, respectively). *Scale bar*, 10 μm. *B*, *top panels*, high magnification sections of the merged images from *A*. *Bottom panels*, fluorescence intensity histograms taken from the indicated region of interest (*ROI*), highlighting the localization of MYPT1/2 (*green line*) in Z-disc and M-band regions under control conditions and redistribution to the A-band region to overlap with sarcomeric MHC (*red line*) after β-adrenergic stimulation.

cytes are terminally differentiated and impossible to propagate and metabolically label in culture (34).

Interplay of Kinases and Phosphatases—A network of kinases and phosphatases regulates the phosphorylation status of the cardiac myofilaments (22, 35). As demonstrated in this study, the myofilament subproteome is simple enough to be interrogated for protein translocation using label-free quantitation. We identified several kinases and phosphatases or related subunits that associate with the cardiac myofibrils and quantified the redistribution of B56α and MYPT1/2 upon β-adrenergic stimulation. The proteomic findings were substantiated by immunoblot analysis of subcellular fractions and by immunolabeling and confocal microscopy.

In our proteomics analysis, several kinases/kinase catalytic subunits that have been shown to target myofilament proteins (*e.g.* protein kinase C isoforms and protein kinase D) were not detected, whereas others (*e.g.* cAMP-dependent protein kinase catalytic subunit and putative myosin light chain kinase 3) were present in the myofilament subproteome (Table II). There are several possible explanations for the absence of certain "myofilament protein kinases" in the subproteome. 1) They may be relatively less abundant. 2) They are only transiently associated with their substrate myofilament proteins. 3) The interaction of these kinases with myofilament proteins is weaker and such that they are lost during the skinning procedure. Interestingly, striated muscle-specific protein kinase (encoded by the striated preferentially expressed gene, SPEG), which has recently been associated with cardiac tropomyosin phosphorylation (36), was also present in the myofilament subproteome in abundance.

Regardless, the actions of kinases that target myofilament proteins upon activation are likely to be counteracted by a range of phosphatases whose own myofilament association may be regulated by dynamic changes in the localization of their regulatory and targeting subunits. Indeed, a defining feature of the two most abundant and extensively studied serine/threonine phosphatase families, PP1 and PP2A, is that they comprise multimeric enzymes with their regulatory/targeting rather than catalytic subunits providing the essential determinants for subcellular localization, substrate specificity, and activity (37). Of the regulatory/targeting subunits whose dynamic myofilament association has been documented in the present study, B56α is a component of the PP2A heterotrimer, whereas MYPT1/2 interact with the catalytic subunit PP1δ, which is also known as myosin phosphatase. As regulatory proteins, B56α and MYPT1/2 do not have catalytic activity themselves, but the observed translocation events are likely to be important in regulating the phosphorylation status of substrates for their catalytic phosphatase partners, such as cTnI for PP2A and MLC-2 for PP1δ. At present, we lack methods to specifically alter the subcellular and intrasarcomeric localization of B56α and MYPT1/2 in response to β-adrenergic stimulation (particularly because isoproterenol would also induce kinase activation). However, our proteomic findings open new avenues for future investigation about the interaction of kinases and phosphatases in the myofilament subproteome (34, 38).

Post-translational Modifications—As noted above, PTMs, notably phosphorylation, play a key role in regulating cardiomyocyte contractility, and the identification of novel PTM sites of myofilament proteins will help to understand the signaling mechanisms that regulate myofilament function. In our study, myofilament proteins from skinned myocytes were separated by gradient SDS-PAGE before analysis by nano-LC MS/MS using the LTQ Orbitrap XL mass spectrometer with CID and ETD measurement in the linear ion trap. Prefractionation by gradient SDS-PAGE separated the myofilament proteins from low abundance proteins, which might otherwise have been masked by the highly abundant components. This approach enabled us to reliably quantify protein translocation based on assigned spectral counts and to even detect phosphopeptides in the myofilament subproteome without enrichment. Importantly, new fragmentation meth-

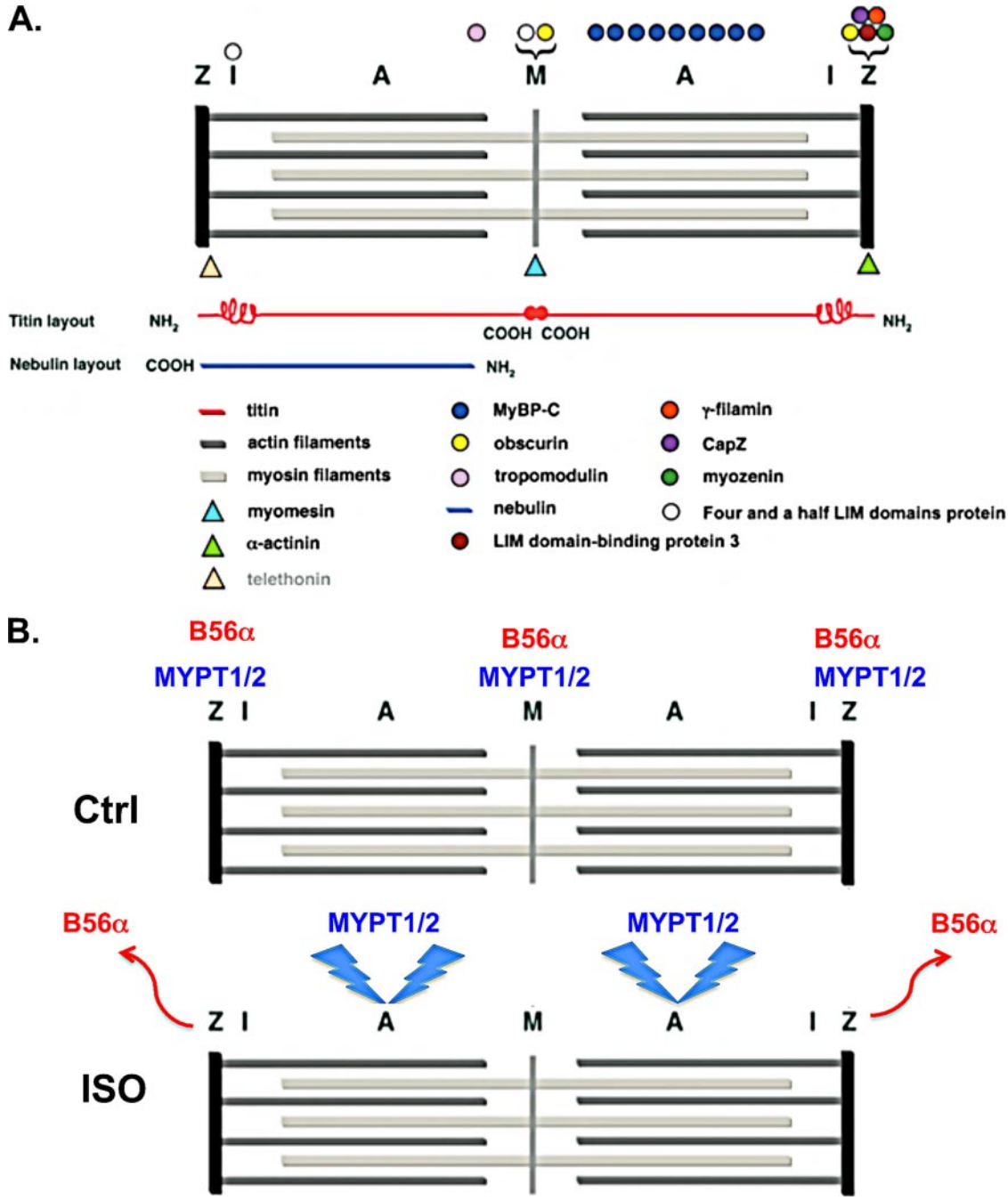

FIG. 9. **Myofilament organization.** *A*, schematic summary of the myofilament proteins identified in this study and their localization within the sarcomere structure. *B*, dissociation of B56α and translocation of MYPT1/2 to sarcomeric MHC upon treatment with isoproterenol. *A*, A-band; *M*, M-band; *Z*, Z-disc; *Ctrl*, control; LIM, Lin-11/Isl-1/Mec3.

ods such as ETD will facilitate the characterization of phosphopeptides, but as evidenced by the presence of numerous sulfated peptides, accurate mass measurement of the precursor ion and/or manual validation of neutral loss ions in linear ion trap CID MS/MS spectra of 98 or 80 is necessary to obtain reliable discrimination of phosphopeptide from sulfopeptide (33). Thus, with the current work flow, accurate mass measurement of the precursor ion readily indicated the nature of the modification with CID as a useful tool for confirmation. The last part of the work flow, ETD, enabled best localization of the site of modification.

Summary—Although to date phosphatases have not attracted the same attention as kinases (39, 40), dynamic changes in their localization and activity are likely to be just as important in the neurohormonal regulation of myofilament protein phosphorylation and therefore cardiac contractility.

This first comprehensive proteomics analysis has revealed the identity of multiple kinases and phosphatases and their related subunits that are associated with the myofilament subproteome and has provided novel information on the dynamic regulation of myofilament-associated phosphatase regulatory subunits that is likely to be of functional significance.

Acknowledgment—We are grateful to Prof. Mathias Gautel for valuable discussions and providing the schematic summary presented in Fig. 9*A*.

* This work was supported by grants from the British Heart Foundation (BHF) and Oak Foundation.

S The on-line version of this article (available at http://www.mcponline.org) contains supplemental Fig. 1 and Tables 1 and 2.

§ Both authors contributed equally to this work.

¶ A Research Councils UK fellow.

‡‡ A senior research fellow of the BHF. To whom correspondence should be addressed: Cardiovascular Division, King's College London, 125 Coldharbour Lane, London SE5 9NU, UK. Tel.: 44-20-7848-5238; Fax: 44-20-7848-5296; E-mail: manuel.mayr@kcl.ac.uk.

REFERENCES

1. Haworth, R. S., Cuello, F., Herron, T. J., Franzen, G., Kentish, J. C., Gautel, M., and Avkiran, M. (2004) Protein kinase D is a novel mediator of cardiac troponin I phosphorylation and regulates myofilament function. *Circ. Res.* **95,** 1091–1099
2. Vahebi, S., Kobayashi, T., Warren, C. M., de Tombe, P. P., and Solaro, R. J. (2005) Functional effects of rho-kinase-dependent phosphorylation of specific sites on cardiac troponin. *Circ. Res.* **96,** 740–747
3. Cuello, F., Bardswell, S. C., Haworth, R. S., Yin, X., Lutz, S., Wieland, T., Mayr, M., Kentish, J. C., and Avkiran, M. (2007) Protein kinase D selectively targets cardiac troponin I and regulates myofilament Ca2+ sensitivity in ventricular myocytes. *Circ. Res.* **100,** 864–873
4. Cazorla, O., Szilagyi, S., Vignier, N., Salazar, G., Krämer, E., Vassort, G., Carrier, L., and Lacampagne, A. (2006) Length and protein kinase A modulations of myocytes in cardiac myosin binding protein C-deficient mice. *Cardiovasc. Res.* **69,** 370–380
5. Stelzer, J. E., Patel, J. R., Walker, J. W., and Moss, R. L. (2007) Differential roles of cardiac myosin-binding protein C and cardiac troponin I in the myofibrillar force responses to protein kinase A phosphorylation. *Circ. Res.* **101,** 503–511
6. Tong, C. W., Stelzer, J. E., Greaser, M. L., Powers, P. A., and Moss, R. L. (2008) Acceleration of crossbridge kinetics by protein kinase A phosphorylation of cardiac myosin binding protein C modulates cardiac function. *Circ. Res.* **103,** 974–982
7. Stelzer, J. E., Patel, J. R., and Moss, R. L. (2006) Acceleration of stretch activation in murine myocardium due to phosphorylation of myosin regulatory light chain. *J. Gen. Physiol.* **128,** 261–272
8. Olsson, M. C., Patel, J. R., Fitzsimons, D. P., Walker, J. W., and Moss, R. L. (2004) Basal myosin light chain phosphorylation is a determinant of Ca2+ sensitivity of force and activation dependence of the kinetics of myocardial force development. *Am. J. Physiol. Heart Circ. Physiol.* **287,** H2712–H2718
9. Scruggs, S. B., Hinken, A. C., Thawornkaiwong, A., Robbins, J., Walker, L. A., de Tombe, P. P., Geenen, D. L., Buttrick, P. M., and Solaro, R. J. (2009) Ablation of ventricular myosin regulatory light chain phosphorylation in mice causes cardiac dysfunction in situ and affects neighboring myofilament protein phosphorylation. *J. Biol. Chem.* **284,** 5097–5106
10. Labugger, R., McDonough, J. L., Neverova, I., and Van Eyk, J. E. (2002) Solubilization, two-dimensional separation and detection of the cardiac myofilament protein troponin T. *Proteomics* **2,** 673–678
11. Zabrouskov, V., Ge, Y., Schwartz, J., and Walker, J. W. (2008) Unraveling molecular complexity of phosphorylated human cardiac troponin I by top down electron capture dissociation/electron transfer dissociation mass spectrometry. *Mol. Cell. Proteomics* **7,** 1838–1849
12. White, M. Y., Cordwell, S. J., McCarron, H. C., Prasan, A. M., Craft, G., Hambly, B. D., and Jeremy, R. W. (2005) Proteomics of ischemia/reperfusion injury in rabbit myocardium reveals alterations to proteins of essential functional systems. *Proteomics* **5,** 1395–1410
13. Yuan, C., Guo, Y., Ravi, R., Przyklenk, K., Shilkofski, N., Diez, R., Cole, R. N., and Murphy, A. M. (2006) Myosin binding protein C is differentially phosphorylated upon myocardial stunning in canine and rat hearts—evidence for novel phosphorylation sites. *Proteomics* **6,** 4176–4186
14. Burkart, E. M., Sumandea, M. P., Kobayashi, T., Nili, M., Martin, A. F., Homsher, E., and Solaro, R. J. (2003) Phosphorylation or glutamic acid substitution at protein kinase C sites on cardiac troponin I differentially depress myofilament tension and shortening velocity. *J. Biol. Chem.* **278,** 11265–11272
15. van der Velden, J., Merkus, D., Klarenbeek, B. R., James, A. T., Boontje, N. M., Dekkers, D. H., Stienen, G. J., Lamers, J. M., and Duncker, D. J. (2004) Alterations in myofilament function contribute to left ventricular dysfunction in pigs early after myocardial infarction. *Circ. Res.* **95,** e85–95
16. van der Velden, J., Narolska, N. A., Lamberts, R. R., Boontje, N. M., Borbély, A., Zaremba, R., Bronzwaer, J. G., Papp, Z., Jaquet, K., Paulus, W. J., and Stienen, G. J. (2006) Functional effects of protein kinase C-mediated myofilament phosphorylation in human myocardium. *Cardiovasc. Res.* **69,** 876–887
17. Yuan, C., and Solaro, R. J. (2008) Myofilament proteins: From cardiac disorders to proteomic changes. *Proteomics Clin. Appl.* **2,** 788–799
18. Jin, W., Brown, A. T., and Murphy, A. M. (2008) Cardiac myofilaments: from proteome to pathophysiology. *Proteomics Clin. Appl.* **2,** 800–810
19. Arrell, D. K., Neverova, I., Fraser, H., Marbán, E., and Van Eyk, J. E. (2001) Proteomic analysis of pharmacologically preconditioned cardiomyocytes reveals novel phosphorylation of myosin light chain 1. *Circ. Res.* **89,** 480–487
20. Syka, J. E., Coon, J. J., Schroeder, M. J., Shabanowitz, J., and Hunt, D. F. (2004) Peptide and protein sequence analysis by electron transfer dissociation mass spectrometry. *Proc. Natl. Acad. Sci. U.S.A.* **101,** 9528–9533
21. Sugden, P. H. (2003) An overview of endothelin signaling in the cardiac myocyte. *J. Mol. Cell. Cardiol.* **35,** 871–886
22. Solaro, R. J. (2008) Multiplex kinase signaling modifies cardiac function at the level of sarcomeric proteins. *J. Biol. Chem.* **283,** 26829–26833
23. Messerli, J. M., Eppenberger-Eberhardt, M. E., Rutishauser, B. M., Schwarb, P., von Arx, P., Koch-Schneidemann, S., Eppenberger, H. M., and Perriard, J. C. (1993) Remodelling of cardiomyocyte cytoarchitecture visualized by three-dimensional (3D) confocal microscopy. *Histochemistry* **100,** 193–202
24. Snabaitis, A. K., D'Mello, R., Dashnyam, S., and Avkiran, M. (2006) A novel role for protein phosphatase 2A in receptor-mediated regulation of the cardiac sarcolemmal Na+/H+ exchanger NHE1. *J. Biol. Chem.* **281,** 20252–20262
25. Sidibe, A., Yin, X., Tarelli, E., Xiao, Q., Zampetaki, A., Xu, Q., and Mayr, M. (2007) Integrated membrane protein analysis of mature and embryonic stem cell-derived smooth muscle cells using a novel combination of CyDye/biotin labeling. *Mol. Cell. Proteomics* **6,** 1788–1797
26. Mayr, M., Chung, Y. L., Mayr, U., McGregor, E., Troy, H., Baier, G., Leitges, M., Dunn, M. J., Griffiths, J. R., and Xu, Q. (2004) Loss of PKCδ alters cardiac metabolism. *Am. J. Physiol. Heart Circ. Physiol.* **287,** H937–H945
27. Yan, J. X., Wait, R., Berkelman, T., Harry, R. A., Westbrook, J. A., Wheeler, C. H., and Dunn, M. J. (2000) A modified silver staining protocol for visualization of proteins compatible with matrix-assisted laser desorption/ionization and electrospray ionization-mass spectrometry. *Electrophoresis* **21,** 3666–3672
28. Shevchenko, A., Wilm, M., Vorm, O., and Mann, M. (1996) Mass spectrometric sequencing of proteins silver-stained polyacrylamide gels. *Anal. Chem.* **68,** 850–858
29. Wilm, M., Shevchenko, A., Houthaeve, T., Breit, S., Schweigerer, L., Fotsis, T., and Mann, M. (1996) Femtomole sequencing of proteins from polyacrylamide gels by nano-electrospray mass spectrometry. *Nature* **379,** 466–469
30. Keller, A., Nesvizhskii, A. I., Kolker, E., and Aebersold, R. (2002) Empirical statistical model to estimate the accuracy of peptide identifications made by MS/MS and database search. *Anal. Chem.* **74,** 5383–5392
31. Nesvizhskii, A. I., Keller, A., Kolker, E., and Aebersold, R. (2003) A statistical model for identifying proteins by tandem mass spectrometry. *Anal.*

Chem. **75,** 4646–4658
32. Perkins, D. N., Pappin, D. J., Creasy, D. M., and Cottrell, J. S. (1999) Probability-based protein identification by searching sequence databases using mass spectrometry data. *Electrophoresis* **20,** 3551–3567
33. Gharib, M., Marcantonio, M., Lehmann, S. G., Courcelles, M., Meloche, S., Verreault, A., and Thibault, P. (2009) Artifactual sulfation of silver-stained proteins: implications for the assignment of phosphorylation and sulfation sites. *Mol. Cell. Proteomics* **8,** 506–518
34. Arrell, D. K., Neverova, I., and Van Eyk, J. E. (2001) Cardiovascular proteomics: evolution and potential. *Circ. Res.* **88,** 763–773
35. Agnetti, G., Kane, L. A., Guarnieri, C., Caldarera, C. M., and Van Eyk, J. E. (2007) Proteomic technologies in the study of kinases: novel tools for the investigation of PKC in the heart. *Pharmacol. Res.* **55,** 511–522
36. Liu, X., Ramjiganesh, T., Chen, Y. H., Chung, S. W., Hall, S. R., Schissel, S. L., Padera, R. F., Jr., Liao, R., Ackerman, K. G., Kajstura, J., Leri, A., Anversa, P., Yet, S. F., Layne, M. D., and Perrella, M. A. (2009) Disruption of striated preferentially expressed gene locus leads to dilated cardiomyopathy in mice. *Circulation* **119,** 261–268
37. Virshup, D. M., and Shenolikar, S. (2009) From promiscuity to precision: protein phosphatases get a makeover. *Mol. Cell* **33,** 537–545
38. Mayr, M., Zhang, J., Greene, A. S., Gutterman, D., Perloff, J., and Ping, P. (2006) Proteomics-based development of biomarkers in cardiovascular disease: mechanistic, clinical, and therapeutic insights. *Mol. Cell. Proteomics* **5,** 1853–1864
39. Mayr, M., Metzler, B., Chung, Y. L., McGregor, E., Mayr, U., Troy, H., Hu, Y., Leitges, M., Pachinger, O., Griffiths, J. R., Dunn, M. J., and Xu, Q. (2004) Ischemic preconditioning exaggerates cardiac damage in PKCδ null mice. *Am. J. Physiol. Heart Circ. Physiol.* **287,** H946–H956
40. Mayr, M., Liem, D., Zhang, J., Li, X., Avliyakulov, N. K., Yang, J. I., Young, G., Vondriska, T. M., Ladroue, C., Madhu, B., Griffiths, J. R., Gomes, A., Xu, Q., and Ping, P. (2009) Proteomic and metabolomic analysis of cardioprotection: Interplay between protein kinase C epsilon and delta in regulating glucose metabolism of murine hearts. *J. Mol. Cell. Cardiol.* **46,** 268–277